

Article

# Marked Enhancement of Roll-Off Frequency in FeCoN Synthetic Antiferromagnetic Films Deposited by Oblique Incidence

Luran Zhang, Dandan Gao, Huan Liu, Jiyang Xie \* and Wanbiao Hu \*

School of Materials Science and Engineering, Yunnan University, Kunming 650091, China

\* Correspondence: xiejyang@ynu.edu.cn (J.X.); huwanbiao@ynu.edu.cn (W.H.);

Tel.: +86-13320582440 (J.X.); +86-13649661962 (W.H.)

Received: 30 June 2019; Accepted: 19 July 2019; Published: 22 July 2019



**Abstract:** A series of FeCoN films were successfully deposited on glass substrates in a magnetron sputtering system. Using oblique incidence method and FeCoN/Ru/FeCoN synthetic antiferromagnetic (SAF) structure, two additional anisotropies energy were introduced: oblique incidence anisotropy and exchange anisotropy energy, which marked enhancement of the effective magnetic anisotropy ( $H_k$ ). The increment of  $H_k$  results in a significant improvement in the roll-off frequency of these films. The roll-off frequency of FeCoN/Ru/FeCoN films with SAF structure can reach up to 8.6 GHz. A feasible approach to conveniently controlling  $H_k$  of soft magnetic thin films by using oblique deposition and SAF structure can further improve their properties for the potential applications in the high frequency region.

**Keywords:** magnetic materials; high frequency properties; synthetic antiferromagnetic; thin films

## 1. Introduction

With the fast development of communication and information technologies, more challenges lie in front of radio-frequency and microwave device designers. Magnetic films with high roll-off frequency ( $f_r$ ) on radio-frequency and microwave applications are required [1,2]. Nowadays, in many devices, the operating frequencies have reached gigahertz bands [3,4]. The  $f_r$  of magnetic thin films used in these devices should be very high, ideally beyond 5 GHz or even 10 GHz. The  $f_r$  is significantly influenced by the effective magnetic anisotropy ( $H_k$ ) and saturation magnetization ( $M_s$ ) of the magnetic film. According to the Landau–Lifshitz–Gilbert (LLG) equation,  $f_r$  is defined as

$$f_r = \frac{\gamma}{2\pi} \mu_0 \sqrt{M_s H_k} \quad (1)$$

where  $\gamma$  is the gyromagnetic factor and  $\mu_0$  is the permeability of vacuum [5].

For obtaining the higher range of ferromagnetic resonance frequency, high saturation magnetization materials with a large effective anisotropy field should be considered. As we know, FeCo alloy with 60–70 at.% Fe shows the highest saturation magnetization (up to 24 kGs) among the metal magnetic materials. But FeCo thin films with isotropic magnetic properties are not applicable for high frequency applications. Many efforts have been adopted to increase the  $H_k$  of FeCo thin films, such as applying an induced magnetic field during film deposition [6], depositing on prestressed substrates [7] or flexible substrates [8], field annealing [9], stress inducing [10], oblique deposition [11], micro strip patterning [12], introducing gradient of the Hf concentration [13,14] and using an organic semiconductors underlayer [15]. However, it is still a big challenge getting a very large  $H_k$  in soft magnetic films and enhancing their  $f_r$  beyond 5 GHz. Besides, FeCo is difficult to achieve good soft

magnetic properties because the FeCo alloy shows a large saturation magnetostriction coefficient (around  $(40\text{--}65) \times 10^{-6}$ ). FeCoN thin film is attracting more and more attentions since its good soft magnetic property and high potential in high-frequency applications [16–19].

In this work, FeCoN single film and FeCoN/Ru/FeCoN synthetic antiferromagnetic (SAF) structure films are produced by using a direct current magnetron sputtering equipment with different oblique angles. Oblique deposition and SAF structure can obviously enhance the  $H_k$  and  $f_r$  of FeCoN films. The films prepared at an increasing oblique angle show an enhancement of the  $H_k$  of FeCoN single and SAF structure films. Magnetic properties, antiferromagnetic behavior and high-frequency performance of the films are discussed.

## 2. Methods

FeCoN (40 nm) film and FeCoN (20 nm)/Ru (0.45 nm)/FeCoN (20 nm) SAF structure films were prepared on glass substrates ( $10 \times 10 \text{ mm}^2$ ) at room temperature by using a direct current magnetron sputtering equipment (Kurt J. Lesker, Jefferson Hills, USA) with a 3-inch  $\text{Fe}_{65}\text{Co}_{35}$  target and a 3-inch Ru target. The schematic diagram of the sputtering arrangement was shown in Figure 1a. The distance between substrate and target was 12 cm. Films were deposited at an oblique angle ( $\theta$ ) ranging from  $0^\circ$  to  $26^\circ$ . A static magnetic field about 600 Oe was applied in the substrate plane which was defined as the easy axis (EA) direction. The sputtering power of FeCoN layer was 50 W and that of Ru interlayer was fixed at 15 W. The low pressure with  $1 \times 10^{-7}$  Torr in the sputtering system was applied. A mixture of Ar and  $\text{N}_2$  (with a flow rate  $f_N = \text{N}_2/(\text{Ar} + \text{N}_2) \times 100\%$ —of 5%), was applied during the sputtering process of FeCoN layers. The sputtering gas during Ru layer deposition was pure Ar. The depositing pressure was 5.0 mTorr. A vibrating sample magnetometer (VSM YP07-VSM-130, Zhongxi, Beijing, China) was utilized to measure the magnetic properties of the films at room temperature. The film electric resistivity at room temperature was measured using the standard four-point measurement technique (ST2263, JGDZ, Suzhou, China). A vector network analyzer (PNA E8363B, Keysight, Santa Rosa, USA) via the microstrip method [20] was introduced to measure the permeability spectra. The composition of films was detected using an energy dispersive spectrometer (EDS, FEL, Hillsboro, USA). The Fe concentration of all films were fixed at  $66 \pm 1\%$ , which changed little with an oblique angle.

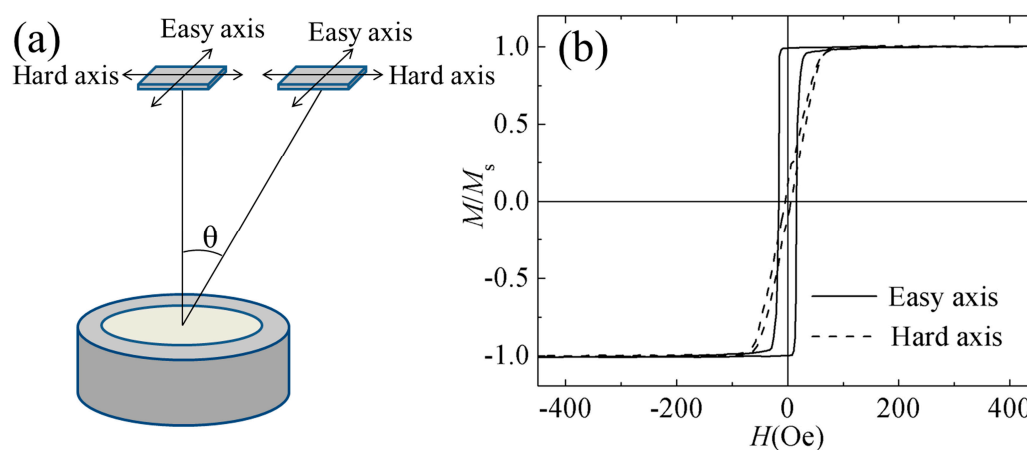


**Figure 1.** (a) Schematic drawing of the sputtering arrangement. (b) Hysteresis loops of single film ( $f_N = 5\%$ ) with oblique angle  $0^\circ$ .

## 3. Results and Discussion

A 5%  $\text{N}_2$  flow ratio was chosen for the FeCoN single layer and SAF structure films because of the high saturation magnetization, low coercivity, and high electric resistivity. The in-plane hysteresis loops of FeCoN single film ( $f_N = 5\%$ ) are shown in Figure 1b. The FeCoN film's saturation magnetization  $4\pi M_s$  is about 21.6 kGs. The EA coercivity  $H_{ce}$ , hard axis (HA) coercivity  $H_{ch}$  and the effective anisotropy

field  $H_k$  of FeCoN film are 15.5 Oe, 5 Oe and 55 Oe respectively. The electric resistivity is  $250 \mu\Omega\cdot\text{cm}$ . The XRD pattern of FeCoN film without oblique angle is shown in Figure 2a. It can be seen that only FeCo (110) peak presents, which means that the FeCoN film shows 110 texture. The FeCo (110) peak is wide and weak, which means that the FeCoN film shows a nanocrystalline structure.

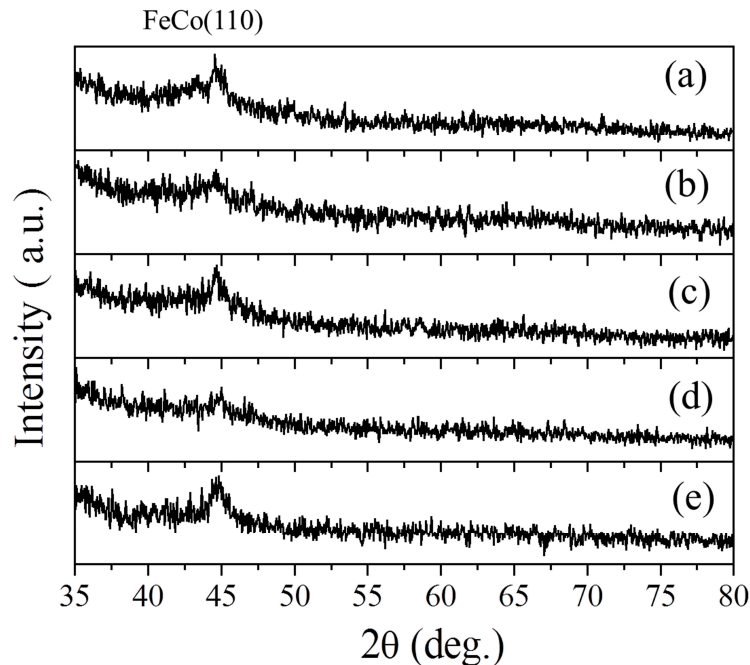


**Figure 2.** XRD pattern of FeCoN single films deposited at oblique angle with  $0^\circ$  (a),  $13^\circ$  (b),  $26^\circ$  (c) and FeCoN SAF films deposited at oblique angle with  $0^\circ$  (d) and  $26^\circ$  (e), respectively.

FeCoN single layer films are deposited at different oblique angle in order to increase the  $H_k$ . The XRD patterns of FeCoN films with oblique angle at  $13^\circ$ ,  $26^\circ$  are shown in Figure 2b,c, respectively. They are not much different to FeCoN film without an oblique angle, only FeCo (110) peak appear. Figure 3a shows the hard axis hysteresis loops of the FeCoN single films deposited at oblique angles of  $0^\circ$ ,  $13^\circ$  and  $26^\circ$ . It is found that the anisotropy increases with an increasing oblique angle. The coercivity of HA are slightly increased under larger oblique angle. The coercivity of EA also increase under larger oblique angle, but much smaller than that of HA. The saturation magnetization is found to be not dependent on position. The  $H_k$  of films are improved gradually with the increment of oblique angle. The  $H_k$  of films prepared with oblique angles at  $0^\circ$ ,  $13^\circ$ ,  $26^\circ$  are 55 Oe, 105 Oe and 160 Oe, respectively. These results reveal that the  $H_k$  of these films rely on the sputtering angle at deposition. The change of effective anisotropy is attributed to an additional anisotropy energy  $K^{\text{oblique}}$  where  $K^{\text{total}} = K^{\text{induced}} + K^{\text{oblique}}$  with  $H_k = 2K^{\text{total}}/M_s$ . According to the Equation (1), the increment of  $H_k$  results in the improvement of the roll-off frequency. As shown in Figure 3b–d, the roll-off frequency of FeCoN single films deposited at oblique angles at  $0^\circ$ ,  $13^\circ$  and  $26^\circ$  are 2.6, 4.1 and 4.7 GHz, respectively.

Figure 4 shows the TEM image of FeCoN single layer film deposited at oblique angle with  $26^\circ$ . It can be seen that the oblique columnar growth of FeCoN. The oblique incidence anisotropy is caused by the columnar growth morphology with the increase of oblique angle [21,22].

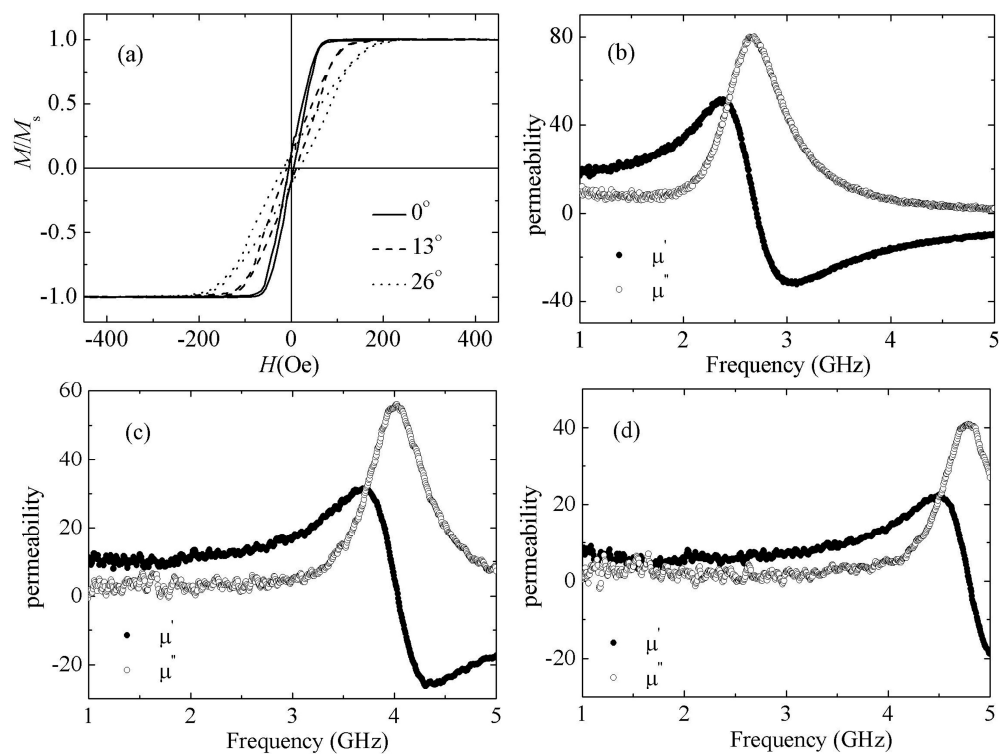


**Figure 3.** Hard axis hysteresis loops (a) and high frequency performance for FeCoN single films deposited at oblique angle with  $0^\circ$  (b),  $13^\circ$  (c) and  $26^\circ$  (d), respectively.

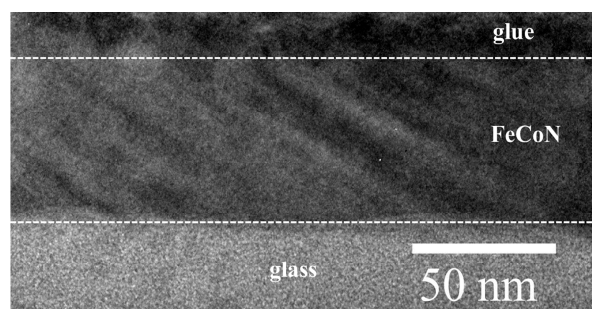


**Figure 4.** Cross section TEM image of FeCoN single layer film deposited at oblique angle with  $26^\circ$ .

To introduce exchange anisotropy, the FeCoN SAF structure films are prepared. In the SAF structure, two ferromagnetic (FM) layers separated by a nonmagnetic (NM) metallic spacer layer have a Ruderman–Kittel–Kasuya–Yosida (RKKY) interaction which is indirect interaction through interlayer exchange coupling [23]. Depending on the thickness, the NM layer can mediate either a ferromagnetic or antiferromagnetic exchange coupling between two FM layers [24]. The XRD patterns of FeCoN SAF structure films with oblique angle at  $0^\circ$  and  $26^\circ$  are shown in Figure 2d,e, respectively. It can be seen that only weak FeCo (110) peak appears. Figure 5a shows the hysteresis loops of FeCoN SAF structure film (glass/FeCoN (20 nm)/Ru (0.45 nm)/FeCoN (20 nm)) with the oblique angle of  $0^\circ$ . The SAF structure film shows distinct separated hysteresis in the EA while the HA loop shows a slanted loop. In the case of a stacked film with interlayer coupling, the magnetization is almost canceled out around the zero field, which means the magnetic moments alignment of the top and bottom magnetic layers are antiparallel. With the increase of the external field, the magnetic moment cancels each other at first. When the external field increases to a certain extent, the magnetic moment reverses. When the external field increases further, the magnetic moments tend to saturate through a rotation-magnetized process. The exchange field ( $H_{ex}$ ) of glass/FeCoN (20 nm)/Ru (0.45 nm)/FeCoN (20 nm) without oblique angle is 80 Oe. Here,  $H_{ex}$  is the smallest field rotating the magnetization in

one of two ferromagnetic layers from the antiparallel alignment. Because of the exchange coupling between the bottom and top magnetic layers, there is an additional anisotropy energy ( $K^{\text{exchange}}$ ) in FeCoN/Ru/FeCoN film, and  $K^{\text{total}} = K^{\text{induced}} + K^{\text{exchange}}$ .  $H_k = 2K^{\text{total}}/M_s$ , so the FeCoN sandwich films'  $H_k$  are larger than that of FeCoN single film. Figure 5c shows the frequency spectrum of FeCoN SAF structure film with the oblique angle of  $0^\circ$ . Compared to the FeCoN single layer film, the roll-off frequency increases from 2.6 to 6.2 GHz. Figure 5b,d shows the hysteresis loops and the high frequency performance of FeCoN SAF structure film with the oblique angle of  $26^\circ$ , respectively. The roll-off frequency of this film drastically increase to 8.6 GHz, which is larger than that of the film prepared without an oblique angle. In this film,  $K^{\text{total}}$  does not only include  $K^{\text{induced}}$ ,  $K^{\text{exchange}}$ , but also includes  $K^{\text{oblique}}$ , so  $K^{\text{total}} = K^{\text{induced}} + K^{\text{exchange}} + K^{\text{oblique}}$ . Therefore, this film's  $H_k$  and the roll-off frequency are larger than that of the film which deposited without an oblique angle. It's should be noticed that the  $H_{\text{ex}}$  of FeCoN sandwich film with oblique angle of  $26^\circ$  is 138 Oe, which is larger than that of the film with  $0^\circ$ . It means FeCoN sandwich film with oblique angle of  $26^\circ$  has larger exchange coupling energy than the film with  $0^\circ$  although they have same structure.

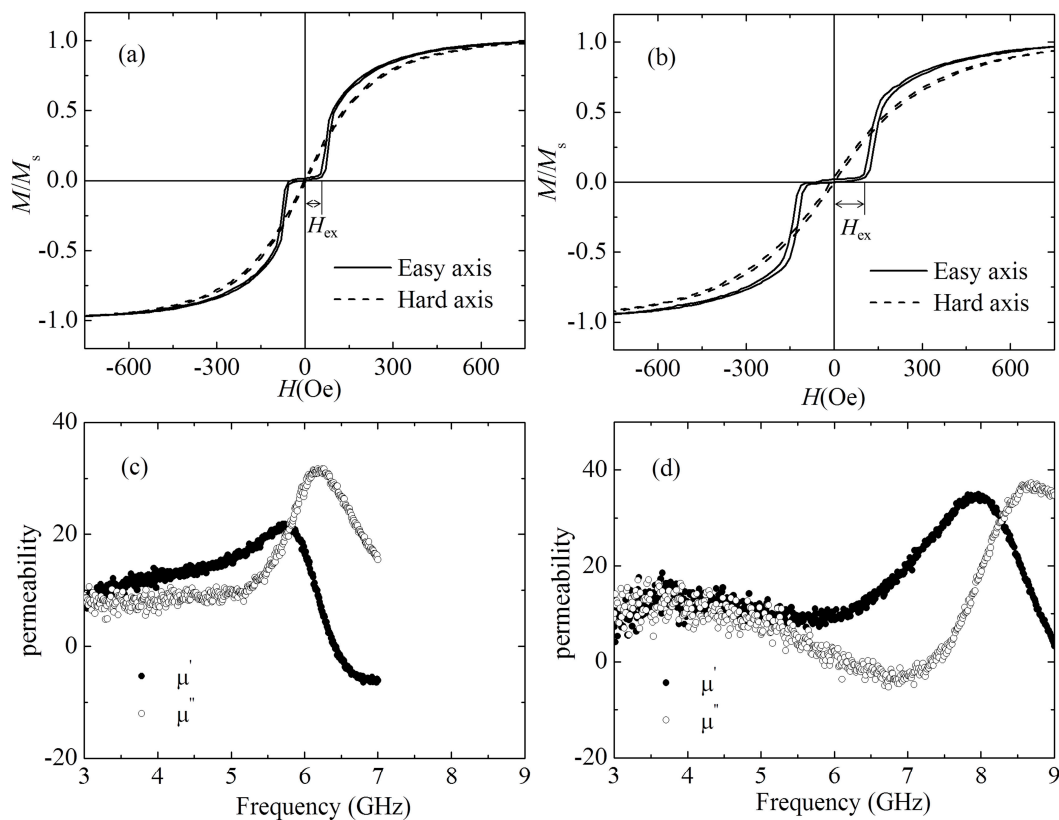


**Figure 5.** Hysteresis loops (a,b) and high frequency performance (c,d) for glass/FeCoN (20 nm)/Ru (0.45 nm)/FeCoN (20 nm) films deposited at oblique angle  $0^\circ$  and  $26^\circ$ , respectively.

#### 4. Conclusion

FeCoN single films and FeCoN/Ru/FeCoN SAF structure films were produced by utilizing a direct current magnetron sputtering equipment under the oblique angles from  $0^\circ$  to  $26^\circ$ . The films deposited with the increase of oblique angle showed an improvement of the  $H_k$  of the FeCoN single and SAF structure films. By using the oblique incidence method and FeCoN/Ru/FeCoN SAF structure, two additional anisotropies energy  $K^{\text{oblique}}$  and  $K^{\text{exchange}}$  are introduced, which can obviously enhance the  $H_k$ . The increase of  $H_k$  results in a significant improvement of the roll-off frequency. The roll-off frequency of FeCoN films were tuned from 2.6 to 8.6 GHz. For the application of soft magnetic thin films with high frequency, controlling the magnitude of  $H_k$  is essential. Compared to other methods

for increasing the  $H_k$  of FeCo thin films, such as depositing on prestressed substrates [7] or flexible substrates [8], micro strip patterning [12], introduces gradient of the Hf concentration [14,15] and using an organic semiconductors underlayer [16], our method is quite simple, more manageable and can get much more higher roll-off frequency. In this work, a feasible approach to conveniently controlling  $H_k$  of FeCoN thin films by using oblique deposition and SAF structure can further improve their properties for the potential applications in the high frequency region.

**Author Contributions:** Conceptualization, L.Z.; methodology, L.Z.; software, L.Z.; validation, L.Z., D.G., H.L., J.X. and W.H.; formal analysis, L.Z.; investigation, L.Z.; resources, L.Z.; data curation, D.G. and H.L.; writing—original draft preparation, L.Z.; writing—review and editing, L.Z.; visualization, J.X. and W.H.; supervision, J.X. and W.H.; project administration, L.Z.

**Funding:** This research received no external funding.

**Conflicts of Interest:** The authors declare no conflict of interest.

## References

1. Luo, M.; Zhou, P.; Liu, Y.; Wang, X.; Xie, J. Electric-Field-Induced Amplitude Tuning of Ferromagnetic Resonance Peak in Nano-granular Film FeCoB-SiO<sub>2</sub>/PMN-PT Composites. *Nanoscale Res. Lett.* **2016**, *11*, 493. [[CrossRef](#)] [[PubMed](#)]
2. Li, Z.; Liu, Y.; Zheng, H.; Zhu, W.; Min, Z.; Zhang, L.; Zhou, P.; Chen, H.; Xin, W.; Lu, H. Thickness-dependent Magnetic and Microwave Resonance Characterization of Combined Stripe Patterned FeCoBSi Films. *Nanoscale Res. Lett.* **2018**, *13*, 97.
3. Zhang, X.; Wang, S.; Zhou, J.; Li, J.; Jiao, D.; Kou, X. Soft magnetic properties, high frequency characteristics, and thermal stability of co-sputtered FeCoTiN films. *J. Alloy. Compd.* **2009**, *474*, 273–278. [[CrossRef](#)]
4. Liu, M.; Li, S.; Duh, J.G. High-frequency ferromagnetic properties of FeNdBO thin films. *J. Alloy. Compd.* **2008**, *455*, 516–518. [[CrossRef](#)]
5. Kittel, C. On the theory of ferromagnetic resonance absorption. *Phys. Rev.* **1948**, *73*, 155. [[CrossRef](#)]
6. Wang, Y.; Zhang, H.; Wen, D.; Zhong, Z.; Bai, F. Magnetic and high frequency properties of nanogranular CoFe-TiO<sub>2</sub> films. *J. Appl. Phys.* **2013**, *113*, 291. [[CrossRef](#)]
7. Fu, Y.; Yang, Z.; Miyao, T.; Matsumoto, M.; Liu, X.X. Morisako, Induced anisotropy in soft magnetic Fe 65 Co 35/Co thin films. *Mater. Sci. Eng. B* **2006**, *133*, 61–65. [[CrossRef](#)]
8. Li, Z.; Sen, Q.; Xing, W.; Jianliang, X.; Longjiang, D. Effect of multilayer structure on high-frequency properties of FeCo/(FeCo)<sub>0.63</sub>(SiO<sub>2</sub>)<sub>0.37</sub> nanogranular films on flexible substrates. *Nanoscale Res. Lett.* **2013**, *8*, 1–4.
9. Tomita, H.; Sato, T.; Mizoguchi, T. Oblique-field annealing effect for in-plane magnetic anisotropy of soft magnetic Co-Nb-Zr thin films. *IEEE Trans. Magn.* **1994**, *30*, 1336–1339. [[CrossRef](#)]
10. Li, S.; Huang, Z.; Duh, J.G.; Yamaguchi, M. Ultrahigh-frequency ferromagnetic properties of FeCoHf films deposited by gradient sputtering. *Appl. Phys. Lett.* **2008**, *92*, 3747. [[CrossRef](#)]
11. Pardavi-Horvath, M.; Ng, B.G.; Castano, F.J.; Korner, H.S.; Garcia, C.; Ross, C.A. Angular dependence of ferromagnetic resonance and magnetization configuration of thin film Permalloy nanoellipse arrays. *J. Appl. Phys.* **2011**, *110*, 053921. [[CrossRef](#)]
12. Zhang, L.; Zheng, H.; Zhu, W.; Li, M.; Zhang, M.; Liu, Y.; Wang, X.; Wang, N.; Harris, V.G.; Xie, J. High frequency magnetic properties of multistriped patterned FeCoBSi thin films. *J. Alloy. Compd.* **2017**, *706*, 318–321. [[CrossRef](#)]
13. Phuoc, N.N.; Le, T.H.; Ong, C.K. FeCoHfN thin films fabricated by co-sputtering with high resonance frequency. *J. Alloy. Compd.* **2011**, *509*, 4010–4013. [[CrossRef](#)]
14. Kuo, C.L.; Li, S.; Duh, J.G. Development and optimisation of FeCoHfN soft magnetic thin films with high-frequency characteristics. *Appl. Surf. Sci.* **2008**, *254*, 7417–7420. [[CrossRef](#)]
15. Wang, Z.; Xu, C.; Wang, J.; Chang, Q.; Zuo, Y.; Li, X. Interface properties of bilayer structure Alq 3/Fe 65 Co 35. *Appl. Surf. Sci.* **2015**, *333*, 119–125. [[CrossRef](#)]
16. Yan, L.; Liu, Z.W.; Tan, C.Y.; Ong, C.K. High frequency characteristics of FeCoN thin films fabricated by sputtering at various (Ar+N<sub>2</sub>) gas flow rates. *J. Appl. Phys.* **2006**, *100*, 3559.
17. Xu, F.; Liao, Z.; Huang, Q.; Chong, K.O.; Li, S. Influence of Sputtering Gas Pressure on High-Frequency Soft Magnetic Properties of FeCoN Thin Film. *IEEE Trans. Magn.* **2011**, *47*, 3921–3923. [[CrossRef](#)]

18. Lu-Ran, Z.; Hua, L.; Xi, L.; Jian-Min, B.; Fu-Lin, W. Excellent soft magnetic properties realized in FeCoN thin films. *Chin. Phys. B* **2012**, *21*, 037502.
19. Hwang, T.J.; Lee, J.; Kim, K.H.; Dong, H.K. Magnetic properties and high frequency characteristics of FeCoN thin films. *Aip Adv.* **2016**, *6*, 146. [[CrossRef](#)]
20. Bekker, V.; Seemann, K.; Leiste, H. A new strip line broad-band measurement evaluation for determining the complex permeability of thin ferromagnetic films. *J. Magn. Magn. Mater.* **2004**, *270*, 327–332. [[CrossRef](#)]
21. KOzawa TYanada HMasuya MSato SIshio, M. Takahashi, Oblique incidence effects in evaporated iron thin films. *J. Magn. Magn. Mater.* **1983**, *35*, 289–292.
22. Jo, S.; Choi, Y.; Ryu, S. Magnetic anisotropy of sputtered FeN films due to anisotropic columnar growth of grains. *IEEE Trans. Magn.* **1997**, *33*, 3634–3636.
23. Liu, X.; Ishio, S.; Ma, H. Study of magnetization reversal process in FeCo/Ru/FeCo exchange coupled synthetic antiferromagnetic multilayers. *J. Nanomater.* **2015**, *2015*, 1–5. [[CrossRef](#)]
24. Li, S.; Wang, C.; Chu, X.M.; Miao, G.X.; Xue, Q.; Zou, W.; Liu, M.; Xu, J.; Li, Q.; Dai, Y. Engineering optical mode ferromagnetic resonance in FeCoB films with ultrathin Ru insertion. *Sci. Rep.* **2016**, *6*, 33349. [[CrossRef](#)] [[PubMed](#)]



© 2019 by the authors. Licensee MDPI, Basel, Switzerland. This article is an open access article distributed under the terms and conditions of the Creative Commons Attribution (CC BY) license (<http://creativecommons.org/licenses/by/4.0/>).